Application of epifluorescence microscopy to the enumeration of aquatic bacterial concentrated on membrane filters

Authors: Gill G. Geesey and J. William Costerton

This is a postprint of a book chapter that originally appeared in Membrane Filtration: Applications, Techniques, and Problems in 1981.

Geesey, G.G. and J.W. Costerton, "Application of Epifluorescence Microscopy to the Enumeration of Aquatic Bacteria Concentrated on Membrane Filters," Membrane Filtration: Applications, Techniques, and Problems, B.J. Dutka (Ed.), Marcel Dekker, Inc., New York, New York, 1981, pp. 253-264.

"Effect of Velocity on Mixed Microbial and Crystallization Cooling Water Fouling of Heat Exchanger Equipment"

ENGINEERING EXPERIMENT STATION

E18001
8/15/81

FINAL REPORT

Chemical Engineering Department - W. G. Characklis

56

ABSTRACT

Fouling in heat exchange equipment can cause significant energy losses as reflected by increased frictional resistance and heat transfer resistance. A model for simulating biofilm development and its influence on heat transfer resistance is described.

Experiments were conducted to measure the deposition of calcium carbonate in the presence of microorganisms (mixed culture) and sodium silicate. Results indicate that the effective roughness of the calcium carbonate deposit is small compared to a biofilm deposit. In addition, sodium silicate and microorganisms both enhance the influence of calcium carbonate deposits on heat transfer resistance.

NOMENCLATURE

A	= wetted surface area	$(L^2t^{-2}T^{-1})$
C_p	= specific heat	$(l^2t^{-2}T^{-1})$
f	= friction factor, $2d\Delta p/L\rho_f Vm^2$	(dimensionless)
h	= convective heat transfer coefficient at r_I	$(Mt^{-3}T^{-1})$
k	= fluid thermal conductivity	$(MLt^{-3}T^{-1})$
k_A	= adsorption rate coefficient	(Lt^{-1})
k'_A	= saturation coefficient	(ML^{-2})
k_B	= thermal conductivity of the Aluminum block	$(MLt^{-3}T^{-1})$
k_{BF}	= apparent thermal conductivity of biofilm	$(MLt^{-3}T^{-1})$
k_D	= detachment rate coefficient	(t^{-1})
k'_D	= coefficient	(Lt^2M^{-1})
k_p	= specific biofilm production rate	(t^{-1})
k'_p	= saturation coefficient	(ML^{-3})
k_s	= thermal conductivity of the deposit	$(MLt^{-3}T^{-1})$
k_t	= thermal conductivity of tube wall material	$(MLt^{-3}T^{-1})$
l	= length of the Aluminum block	(L)
L	= distance between pressure parts	(L)
N	= rate of nutrient consumption by biofilm	$(ML^{-2}t^{-1})$
q	= heat transferred to the Aluminum block	(ML^2t^{-3})
r	= radial distance	(L)
r_1	= inner radius of tube	(L)
r_2	= outside radius of tube	(L)
r_i	= radial distance to inner thermistor of TWHE	(L)
r_{ii}	= radial distance to outer thermistor of TWHE	(L)
r_I	= radial distance to the biofilm	(L)
R_A	= net rate of transport and adsorption of cells, organic and inorganics to the surface	$(ML^{-2}t^{-1})$
R_B	= net biofilm accumulation rate	$(ML^{-2}t^{-1})$
R_D	= rate of detachment of biofilm	$(ML^{-2}t^{-1})$

R_f	= fouling resistance	$(M^{-1}t^3T)$
s	= limiting nutrient concentration in bulk water	(ML^{-3})
T_1	= temperature at r_1	(T)
T_i	= temperature in tube wall at r_i	(T)
T_{ii}	= temperature in tube wall at r_{ii}	(T)
T_b	= bulk fluid temperature	(T)
$T_{B(avg)}$	= average bulk fluid temperature	(T)
Th	= biofilm thickness	(L)
T_I	= temperature at r_I	(T)
U^{-1}	= overall heat transfer resistance	$(M^{-1}t^3T)$
U_o^{-1}	= overall heat transfer resistance at time zero	$(M^{-1}t^3T)$
U_{cond}^{-1}	= conductive heat transfer resistance	$(M^{-1}t^3T)$
U_{cond}^{-1}	= convective heat transfer resistance	$(M^{-1}t^3T)$
U_{cond}^{-1}	= overall heat transfer resistance	$(M^{-1}t^3T)$
v_m	= mean fluid velocity	(Lt^{-1})
x	= biomass concentration in bulk water	(ML^{-3})
Y	= mass of biofilm produced per unit nutrient mass consumed	(dimensionless)
z	= length	(L)
Δp	= pressure drop across length L	$(ML^{-1}t^{-2})$
u	= fluid viscosity	$(ML^{-1}t^{-1})$
ρ_f	= fluid density	(ML^{-3})
ρ	= biofilm density	(ML^{-3})
t_w	= fluid shear stress at biofilm surface	$(ML^{-1}t^{-2})$
δ_1	= viscous sublayer thickness	(L)
ε	= effective height of roughness element	(L)

INTRODUCTION

The term fouling refers to the undesirable formation of inorganic and/or organic deposits on surfaces. These deposits can impede the flow of heat across the surface, increase the fluid frictional resistance at the surface, and increase the rate of corrosion at the surface. In each case, energy loss results.

Fouling Deposits

Several types of fouling and their combinations may occur in heat exchangers: (1) crystalline or precipitation fouling, (2) corrosion fouling, (3) particulate fouling, (4) chemical reaction fouling, and (5) biological fouling or biofouling. Biological fouling results from (a) development of an organic film (biofilm) consisting of microorganisms and their products (microbial fouling), (b) deposition and growth of macroorganisms such as barnacles (macrobial fouling), and (c)assorted detritus. Although many different macroorganisms such as barnacles and mussels have been identified in fouling communities, this paper will concentrate on microbial fouling assuming that it always precedes colonization of the surface by macroorganisms. Based on this premise, control of microbial fouling results in control of macrobial fouling.

Biofouling is not limited to microbial activity. The term includes the interaction of the microorganisms and the slime layer with both the chemistry of the solid surface and the bulk fluid. The interaction can enhance some of the more commonly known phenomena such as precipitation or crystallization (scaling) and corrosion. The rate and extent of fouling due to various mechanisms will partially be determined by transport processes and the physical properties of the resulting fouling deposits (e.g., thermal conductivity, rheological properties, roughness). There can be no doubt that fouling biofilms that form on condenser surfaces reduce heat transfer and lower plant efficiency. Parkiss (1) observed

a decrease of nearly 80% in the performance of a cooling system over a seven week period due to biofouling. Ritter and Suitor (2) measured fouling resistance in six power plant condensers of 240 MW design capacity and estimated the cost of extra fuel for this system due to fouling was $350,000 (1976 dollars). Other documentation related to the costs of fouling is presented elsewhere (3).

Process Description

Development of a systematic understanding of biofouling from field observations has been limited because of the interaction of several contributing rate processes. Mechanistically, fouling biofilm assumulation may be described as the net result of the following (Figure 1):

- Transport of material from the bulk fluid to the surface and adhesion to the surface. Transported materials can be soluble (microbial nutrients and organic salts) or particulate (viable microorganisms, their detritus, or inorganic particles). Fouling begins once these materials adhere to the surface. Suspended particles of sufficient mass may also control films by "scouring" action.

- Microbial reactions within the film. Microbial growth in the biofilm and extracellular polymers produced by the microorganisms contribute to biofilm accumulation and promote adherence of inorganic suspended solids.

- Fluid shear stress at the surface of the film. Such forces can limit the overall extent of the fouling deposit by removing attached material.

- Surface material and roughness. Surface properties can influence micromixing near the surface and corrosion processes. Some metal surfaces may release toxic components into the biofilm inhibiting growth and/or attachment. Some metals produce loosely held oxide films under the biofilms. When the oxide film sloughs, the biofilm is also removed.

- Fouling control procedures. Chlorine, the most commonly used chemical, oxidizes biofilm polymers causing disruption and partial removal of biofilm in the fluid shear stress field. Inactivation of a portion of the microbial population also occurs. Altered biofilm "roughness" and decreased viable cell numbers influence "regrowth" rates of the biofilm. Mechanical cleaning physically removes a portion of the attached film.

Effects of Fouling

Fouling deposits can cause the following deleterious effects in heat exchangers:

- increased fluid frictional resistance

- increased overall heat transfer resistance

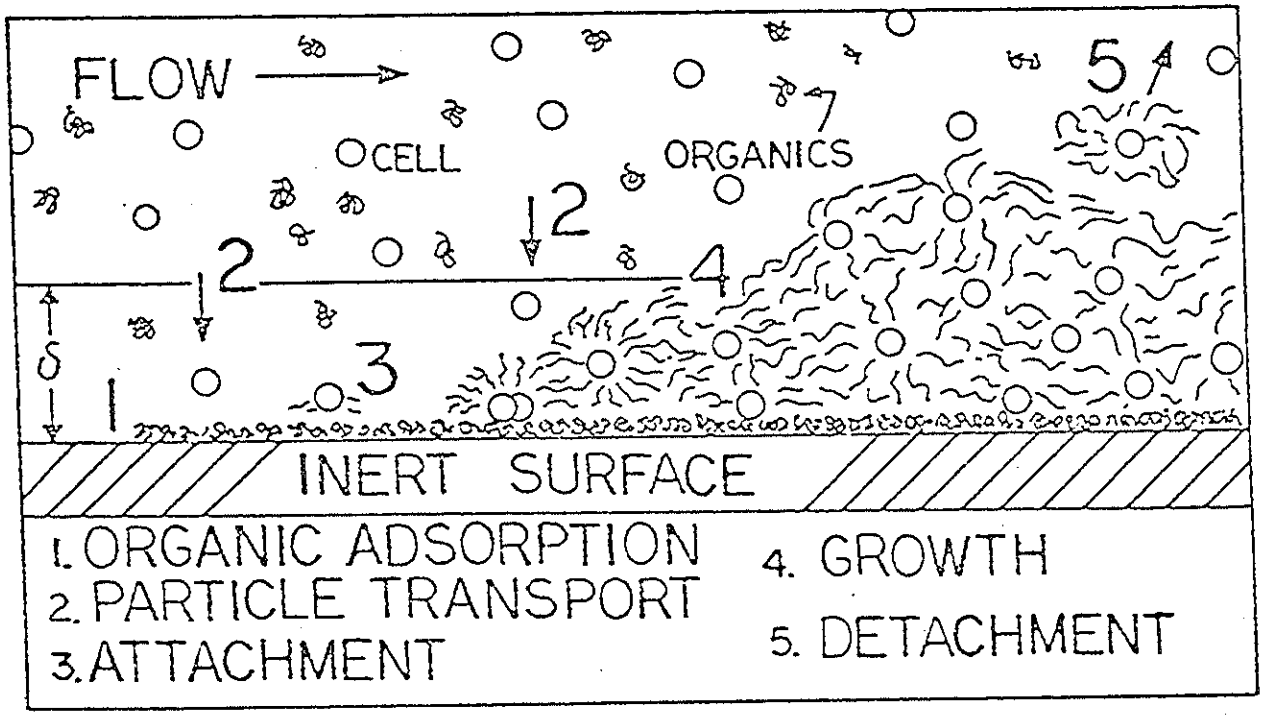

Figure 1. Summary Diagram of the Biofouling Processes.

Fouling deposits cause increased fluid frictional resistance by decreasing the effective diameter of the heat exchange tube and by increasing the tube roughness. Picologlou et.al. (4) have indicated that biofilms increase frictional resistance primarily by increasing the effective roughness of the tube.

Overall heat transfer resistance is the sum of conductive and convective heat transfer resistances. Convective heat transfer resistance will decrease as fouling progresses due to the increased turbulence resulting from deposit formation. However, conductive heat transfer resistance will increase as the insulating fouling deposit accumulates. The relative changes in convective and conductive heat transfer resistance will depend on the following:

- thickness, roughness and thermal conductivity of the deposit
- fluid flow rate
- wall temperature of the clean tube

Characklis et.al. (5) have reported the influence of fouling biofilm on conductive and convective heat transfer resistance in tubes in a laboratory system.

MATHEMATICAL SIMULATION OF BIOFOULING IN A CIRCULAR TUBE

A mathematical model simulating fouling biofilm development and its influence on heat transfer will be described. The model may be useful for several purposes including the following (6):

- Economical experimentation - fouling processes can be studied more quickly and economically than possible in the laboratory or field.
- Extrapolation - extreme ranges of operating conditions can be tested which may be impractical otherwise.
- Evaluation of alternative policies - various designs, operating procedures and treatment processes can be tested before decisions are made.
- Design of experiments - the model indicates the variables to be measured and the data that must be provided for useful evaluation procedures.
- Test of sensitivity - the model can indicate which parameters have a significant influence on process behavior.

However, one significant limitation of modelling must be recognized. The success of the model depends heavily on the basic information available. The model is only as accurate as the physical, chemical, and biological data that go into the model.

Model Component 1: Fouling Biofilm Development

Fouling biofilm development is the net result of several physical, chemical and biological processes including the following:

- transport and adsorption of inorganic and organic molecules at the wetted surface
- transport of microbial cells and other particulate material to the wetted surface
- adsorption and microbial adhesion to the surface
- microbial reactions within the biofilm
- detachment of portions of the deposit by fluid shear

Net biofilm accumulation rate, R_B, reflects a combination of all the rate processes above:

$$R_B A = R_A A = NAY - R_D A \qquad (1)$$

where R_A = net rate of transport and adsorption of cells, organics and inorganics on the surface $(ML^{-2}t^{-1})$

R_D = rate of detachment of biofilm $(ML^{-2}t^{-1})$

N = rate of nutrient consumption by the biofilm $(ML^{-2}t^{-1})$

A = wetted surface area (L^2)

Y = mass of biofilm produced per unit nutrient mass consumed (dimensionless)

Net rate of transport and adsorption has been described (7) as follows:

$$R_A = k_A \times (1 - \frac{\rho Th}{k'_A}) \qquad (2)$$

where x = biomass concentration in bulk water (ML^{-3})

ρ = biofilm density (ML^{-3})

Th = biofilm thickness (L).

k_A = adsorption rate coefficient (Lt^{-1})

k'_A = saturation coefficient (ML^{-2})

The rate of biofilm production due to nutrient consumption, N Y, has been experimentally determined by Trulear and Characklis (8) as follows:

$$NY = \frac{k_p \rho Th\ s}{k'_p + s} \qquad (3)$$

where k_p = specific biofilm production rate (t^{-1})

s = limiting nutrient concentration in bulk water (ML^{-3})

k'_p = saturation coefficient (ML^{-3})

The rate of biofilm detachment due to fluid shear, R_D, has been experimentally determined by Trulear and Characklis (8). An approximate expression can be derived from their data as follows:

$$R_D = \rho Th\ k_D \exp(k'_D \tau_w) \qquad (4)$$

where t_w = fluid shear stress at the biofilm surface $(ML^{-1}t^{-2})$

k_D = detachment rate coefficient (t^{-1})

k'_D = coefficient (Lt^2M^{-1})

Model Component 2: Fluid Frictional Resistance

Picologlou et.al. (4) have experimentally determined the influence of biofilm on fluid frictional resistance. Friction factor, f, was independent of Reynolds number, Re, for Re > 10,000 when Th exceeded the viscous sublayer thickness, δ_1. However, f was a function of biofilm roughness, ε. Therefore, the following expression describes the dimensionless friction factor (f) in a tube where $Th > \delta_1$ (Davies (9)):

$$f = \left[1.13 - 0.87 \ln\left(\frac{\varepsilon}{2r_I}\right)\right]^{-2} \qquad (5)$$

where ε = effective height of roughness elements (L)

$r_I = (r_1 - Th)$ = effective tube radius (L)

r_1 = tube radius (L)

Friction factor for any thickness and roughness is described by:

$$f = \frac{4r_1}{L} \frac{\Delta p}{\rho_f v_m^2} \quad (6)$$

where Δp = pressure drop across tube length L $(ML^{-1}t^{-2})$

L = tube length (L)

v_m = mean fluid velocity (Lt^{-1})

ρ_f = fluid density (ML^{-3})

Model Component 3: Conductive Heat Transfer Resistance

The conductive heat transfer resistance due to biofilm, U_{cond}^{-1}, and biofilm thermal conductivity, k_{BF} were determined by Characklis et.al. (5). Then

$$U_{cond}^{-1} = \frac{r_I}{k_{BF}} \ln \frac{r_1}{r_I} \quad (7)$$

where k_{BF} = biofilm thermal conductivity $(MLt^{-3}T^{-1})$

Model Component 4: Convective Heat Transfer Resistance

Colburn (10) proposed a relationship to predict convective heat transfer coefficient from friction factor:

$$h = 0.125\ f\ C_p^{0.33}\ \mu^{-0.67}\ k^{0.67}\ \rho_f\ v_m \quad (8)$$

where h = convective heat transfer coefficient $(Mt^{-3}T^{-1})$

C_p = specific heat of the fluid $(L^2t^{-2}T^{-1})$

μ = fluid viscosity $(ML^{-1}t^{-1})$

k = fluid thermal conductivity $(MLt^{-3}T^{-1})$

Then convective heat transfer resistance, $U_{conv}^{-1} = \frac{r_i}{r_I} \frac{1}{h}$

Model Component 5: Overall Heat Transfer Resistance

The overall heat transfer residence, $U_{overall}^{-1}$, is the sum of conductive resistance and convective resistance.

$$U_{overall}^{-1} = U_{cond}^{-1} + U_{conv}^{-1} \quad (9)$$

A flow diagram of the model describing biofilm development in a tube and its influence on overall heat transfer resistance is presented in Figure 2.

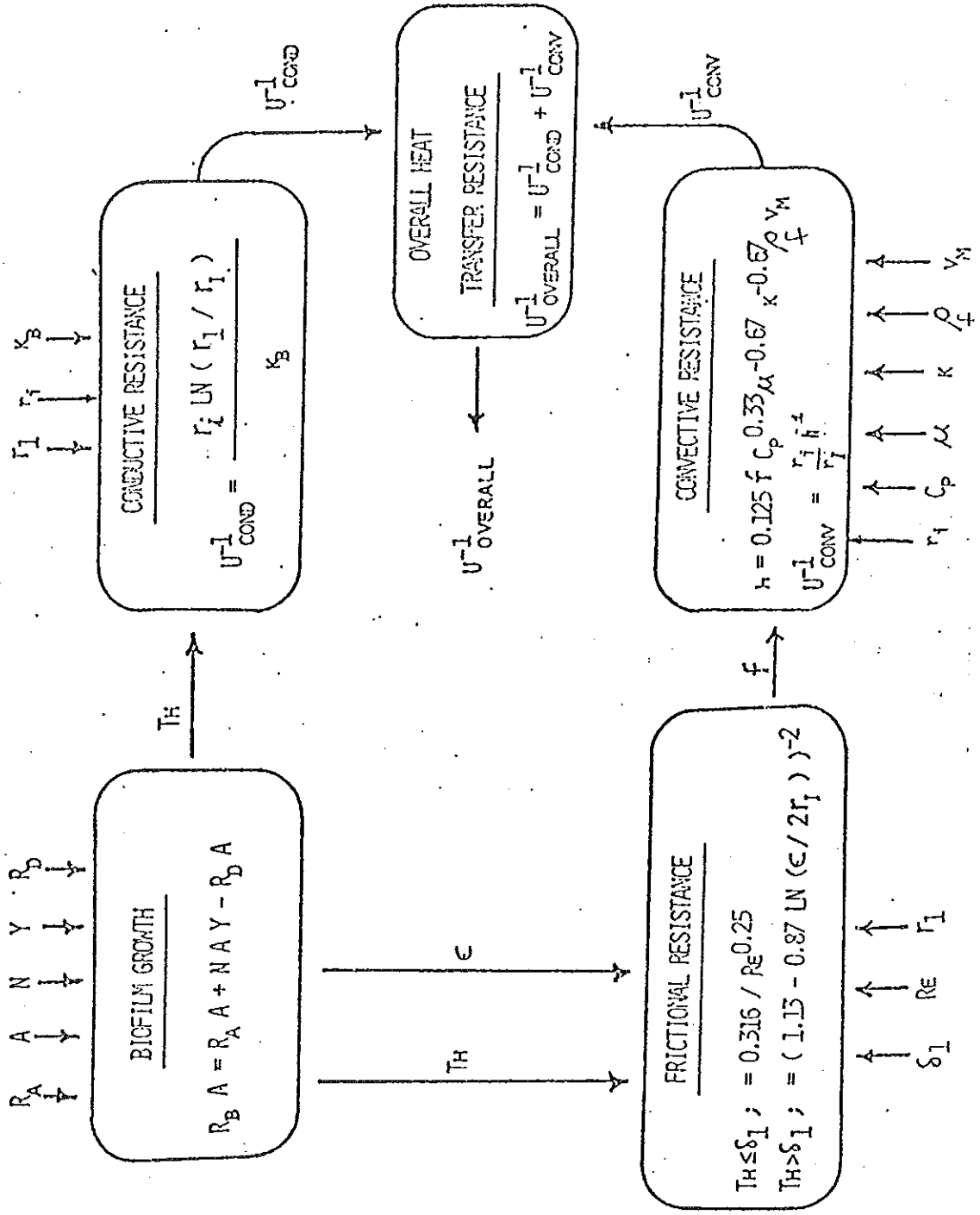

Figure 2. Biofilm Development and Heat Transfer Resistance Model.

EXPERIMENTAL APPARATUS AND METHODS

The Tubular Fouling Monitor

A simplified flow diagram of the experimental setup is shown in Figure 3. It essentially consists of three major components (Figure 4):

1. The tubular reactor contains a heat transfer section consisting of an electrically heated aluminum block clamped around the tube. Two thermistor are embedded in the aluminum block (TWHE) at two different radial distances from the center of the tube. The tube is interchangeable and can be made up of any alloy. The tube contains parts for pressure drop measurements. The pressure drop across the TWHE is measured by a Validyne differential pressure transducer system. The reactor also includes a flow meter, and two temperature probes for measuring bulk water temperature.
2. An Apple II plus microcomputer serves as a complete data processing unit for the tubular reactor. From the data collected from the tubular reactor, it calculates friction factor and the overall heat transfer resistance. Output from the microcomputer includes a television monitor for continuous display and a cassette recorder to establish historic record.
3. A micrometer device to measure the thickness of the deposit. The thickness is measured in a sectioned aluminum block having five ports. The micrometer has a contact probe, which is insulated except the tip. The micrometer arm is slowly lowered in the port until a contact is made between the contact probe and the clean tube. The micrometer reading is noted. The final reading between the fouled tube and the contact probe is noted. The difference in micrometer reading determines the deposit thickness.

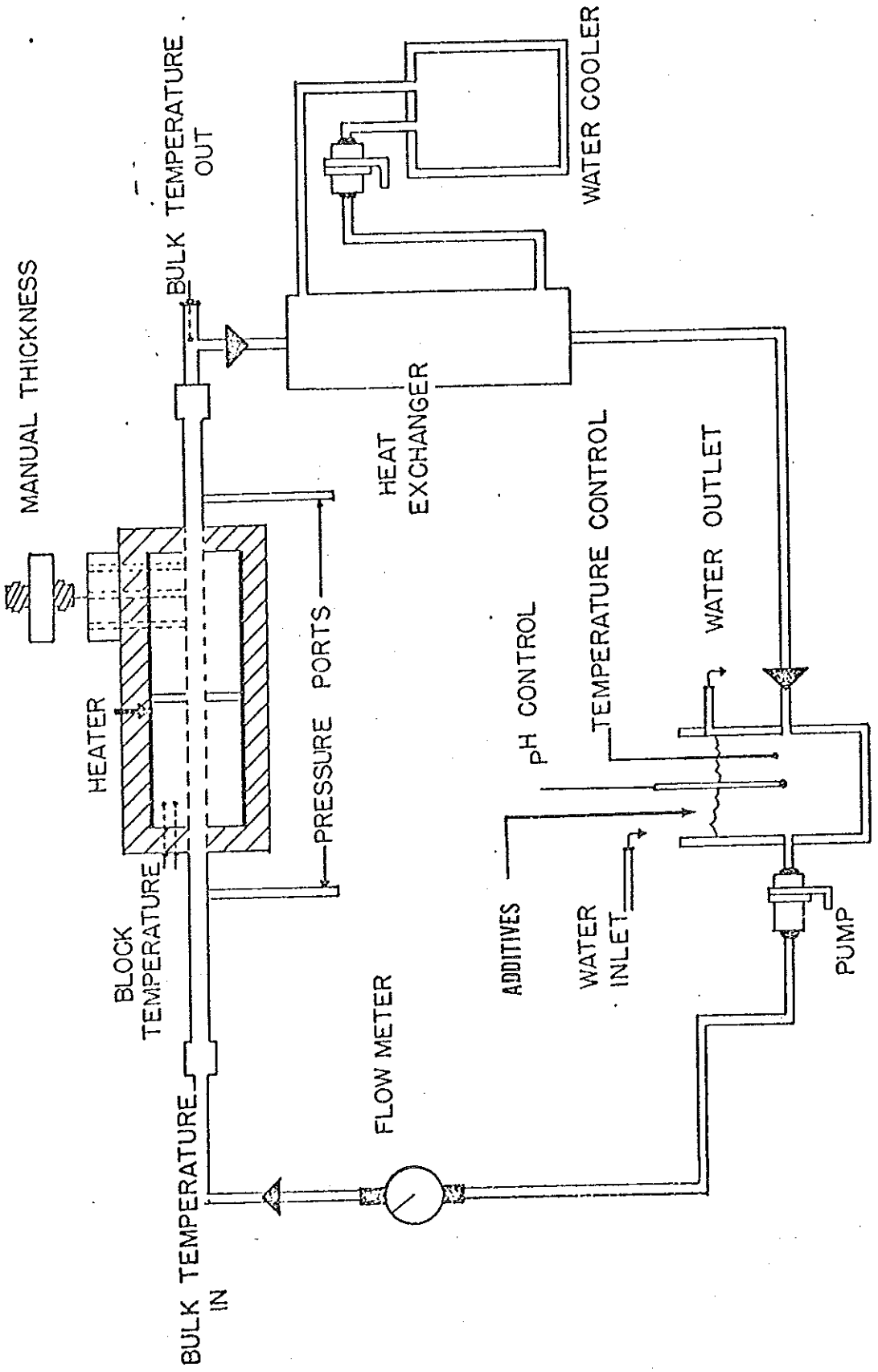

Figure 3. Flow Diagram of the Tubular Fouling Monitoring System.

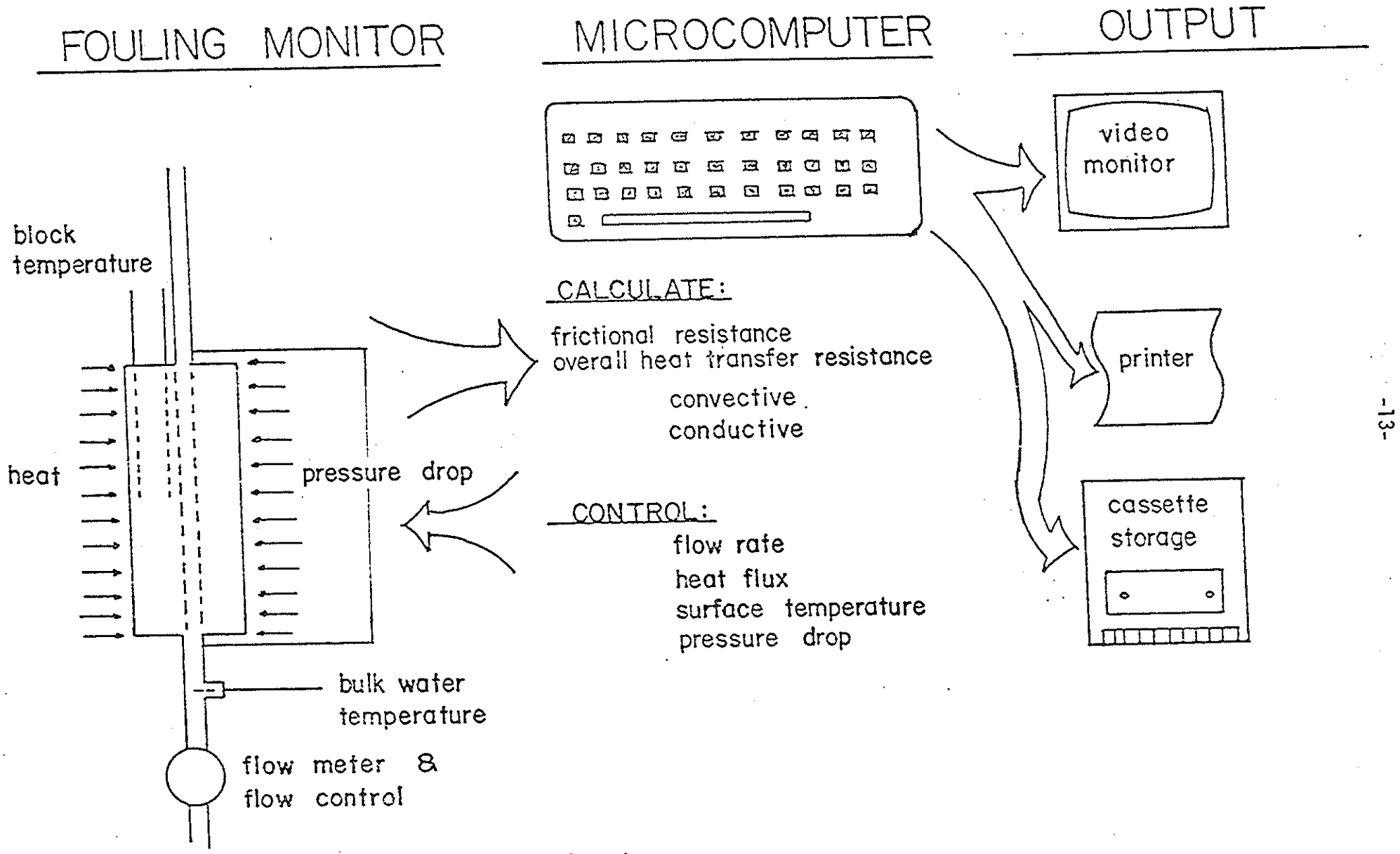

Figure 4. Fouling Monitoring System.

Experimental Methods

Experiments were conducted to study the deposition of calcium carbonate in presence of microorganisms (mix culture) and sodium silicate. Table 3 gives a summary of the experimental work.

These experiments were operated at constant heat flux, constant velocity and constant bulk water temperature using simulated cooling water. All the experiments were started with a clean 1.27 cm ID, 70:30 CuNi tube.

The flow diagram of the experimental system is as shown in Figure 3. The bulk temperature was kept constant at 35°C by controlling the flow of cooling water (using selonids values) in the concentric tube heat exchanger. The pH of the simulated water was held constant at 8-8.2.

Since calcium carbonate is insoluble in neutral water, it was dissolved in concentrated hydrochloric acid. The calcium carbonate solution was fed to the system by gravity. Sodium silicate was dissolved in 0.125% sodium hydroxide and fed by gravity. Distilled water was used as dilution water. TSB (Trypticase soya broth, 5 ml/l) was used as a substrate for microorganisms. Overall heat transfer resistance was calculated from bulk water temperature and the temperature in the aluminum block. Friction factor was determined from pressure drop and flow measurement in the tubular sections.

Tube samples (at the end of Run 7) were obtained from heat transfer measurement block, thickness measurement block, and unheat section. The dry ° mass (65°C for 3 hrs.) of the deposit was calculated and is reported in Table 5.

RESULTS

Heat Transfer Resistance

Figure 5 is a schematic diagram of the TWHE with a fouled surface heated at a constant rate. By measuring the temperature at the two radial positions within the aluminum block (r_i and r_{ii}), the heat transferred to the block can be obtained

$$q = \frac{2\pi k_B l\ (T_{ii} - T_l)}{\ln\ (r_{ii}/r_i)} \qquad (10)$$

where k_B = thermal condictivity of Aluminum block $(MLt^{-3}T^{-1})$

l = length of the block (L)

Heat transfer rate in a tube is generally described in terms of an overall heat transfer coefficient (U). The inverse of the overall heat transfer coefficient (U) is the overall heat transfer resistance.

The overall heat transfer resistance (based on average bulk fluid temperature) can be obtained as

$$U^{-1} = \frac{2\pi r_i l\ (T_i - T_{B(avg)})}{q} \qquad (11)$$

where $T_{B(avg)}$ = average bulk fluid temperature = $\frac{T_{B1} + T_{B2}}{2}$

U^{-1} = overall heat transfer resistance $(M^{-1}L^3T)$

The influence of the deposit on heat transfer resistance can be also expressed as

(a) Fouling resistance

(b) Performance index

The fouling resistance, R_f, is defined as follows:

$$R_f = U^{-1} - U_o^{-1} \qquad (12)$$

where R_f = fouling factor (t^3TM^{-1})

U = overall heat transfer coefficient at any time $(Mt^{-3}T^{-1})$

U_o = overall heat transfer coefficient at time t=0 $(Mt^{-3}T^{-1})$

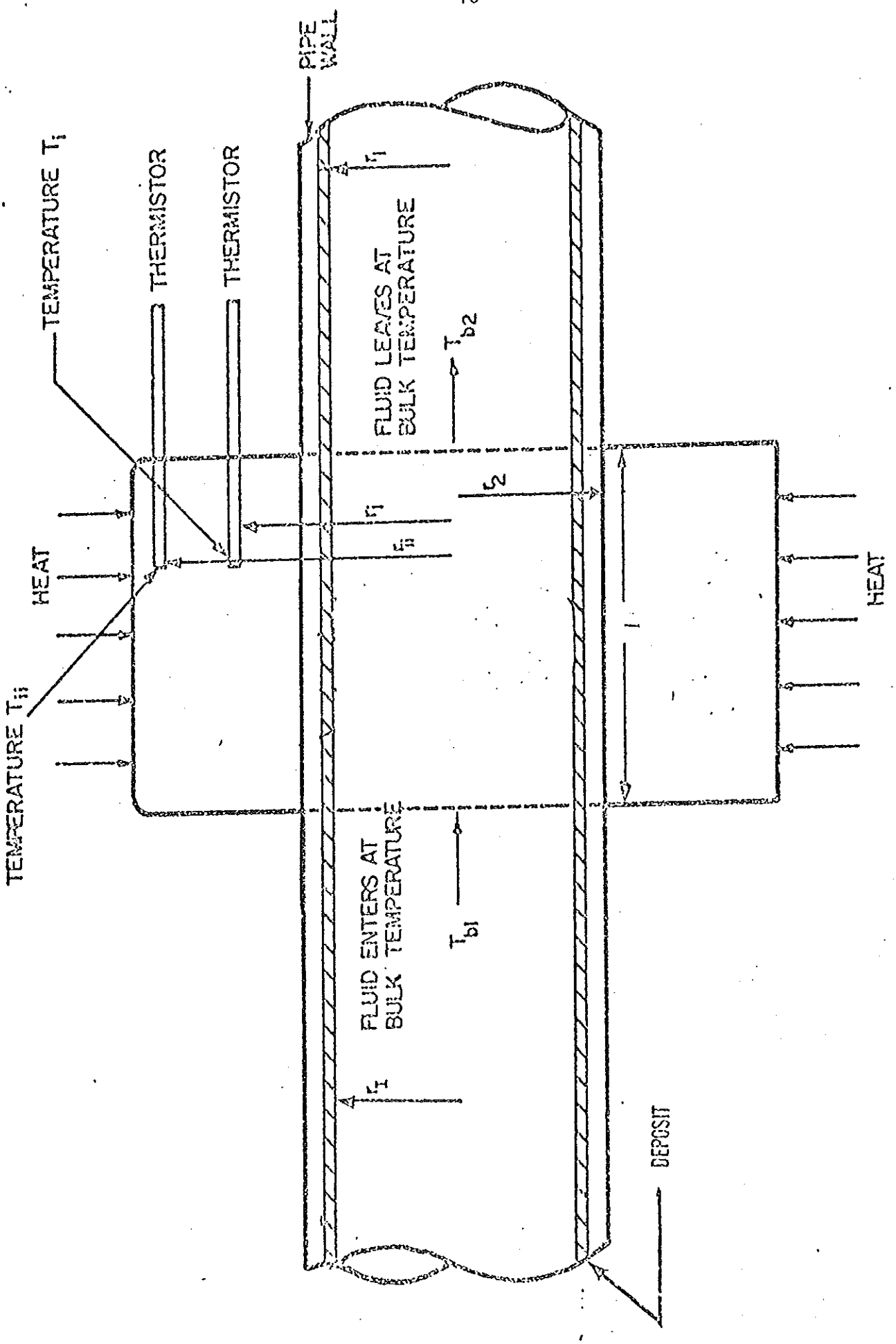

Figure 5: Cross-sectional Diagram of the Tubular Reactor.

These two heat transfer coefficients can also be used as a measure of heat exchanger performance (11):

$$\text{Performance Index} = \frac{U}{U_o}(\%) \qquad (13)$$

During the start of the experiment with a clean tube, the performance index is expected to be 100. The index decreases as the surface fouls.

Frictional Resistance

Frictional resistance is determined from the pressure drop and flow measurement in the tubular section and is calculated by:

$$f = \frac{4r_1}{L} \frac{\Delta_p}{\rho_f V_m^2} \qquad (6)$$

Overall Heat Transfer Resistance

Overall heat transfer resistance is calculated from measurements of bulk water temperature and temperature in the sluminum block. Overall heat transfer resistance is sum of conductive and convective heat transfer resistances:

$$U^{-1} = \frac{r_i}{r_I}\frac{1}{h} + \frac{r_i \ln (r_i/r_i)}{k_s} + \frac{r_i \ln(r_2/r_1)}{k_T} + \frac{r_i \ln(r_i/r_2)}{k_B} \qquad (14)$$

convective ←——————CONDUCTIVE RESISTANCES——→

resistance

where k_B = thermal conductivity of Aluminum block

k_T = thermal conductivity of tube

k_S = thermal conductivity of deposit

$r_I = r_1 - Th$ = radial distance to the deposit

h = convective heat transfer coefficient

The convective heat transfer coefficient can be calculated using Colburn anology (Equation 8). Equation 14 can be used to calculate the thermal conductivity of the deposit, provided the thickness of the deposit is measured. A comparison of the thermal conductivities for the biofilm and scale is shown in Table 1. The difference is thermal conductivities suggests an effective method for distinguishing between scale and biofilm and hence their treatments (Table 2).

RESULTS & DISCUSSION

The fouling monitor was operated in the laboratory using simulated cooling water. All the experiments were operated at constant heat flux, constant velocity, and constant bulk water temperature. The experimental results are expressed in the form of overall heat transfer resistance and friction factor, as a function of time (Figures 6 through 11). The following observations are worthy of note:

1. Results indicate the effective roughness of $CaCO_3$ is small compared to biofilms (Table 4).

2. The dilution water contains no or little inert suspended solids. Suspended solids in cooling water can significantly influence deposit accumulation in a tube.

3. The microbial inoculum was composed of a variety of microbial species. A plate count during the experiment shows a viable cell count of $_{10}6$ cell/ml. Microbial population in cooling water will be site specific.

4. Microorganisms appear not to attach to a heated tube (temperature greater then 55°C). This was observed during Run 5 (Figure 8), where there was little or no increase in overall heat transfer resistance in 117 hours.

5. These experiments were carried out in a 70:30 CuNi tube. This alloy corrodes at the surface in addition to the crystallization of calcium carbonate.

6. There was no correlation observed between heat transfer and frictional resistance measurements (Figure 6 and Figure 7).

SUMMARY

A brief review of different types of deposit is presented. Biofilm development and its influence on fluid frictional resistance and heat transfer resistance has been described in conceptual and mathematical model.

A fouling monitoring system has been described. Thermal conductivity and relative roughness of the deposit can provide useful insight to distinguish between the scale and biofilm. Further work is needed to study (1) the interaction of calcium carbonate and microorganism at heat transfer surface (2) the role of inorganic components (eg, Fe, Si) in fouling initation.

REFERENCES

1. Purkiss, B.E., "Biotechnology of Industrial Water Conservation," M & B Monographs, Mills and Boon, London (1972).

2. Ritter, R.B. and Suitor, J.W., "Fouling Research on Copper and Its Alloys - Seawater Studies, " HTRI Progress Report, INCRA Project No. 214A, April 1976.

3. Somerscales, E.F.C. and Knudsen, J.G., "Fouling of Heat Transfer Equipment," Hemisphere Publishing Co., Washington (1979).

4. Picologlou, B.F., Zelver, N. and Characklis, W.G., "Biofilm Growth and Hydraulic Performance," J. Hyd. Div., Proc. ASCE, vol. 106, no. HY5, 1980, p. 733.

5. Characklis, W.G., Nimmons, M.J., and Picologlou, B.F., "Biofilm Development and Heat Transfer," accepted by Heat Transfer Engineering, 1981.

6. Himmelblau, D.M., and Bischoff, K.B.,"Process Analysis and Simulation, " John Wiley and Sons, New York, 1968.

7. Fletcher, M., "The Effect of Culture Concentration and Age, Time, and Temperature on Bacterial Attachment to Polystyrene," Canadian Journal of Microbiology, vol. 23, 1977, pp. 1-6.

8. Trulear, M.G., Characklis, W.G., "Dynamics of Biofilm Processes," accepted for publication, Journal Water Polution Control Federation, 1981.

9. Davies, J.T.,"Turbulence Phenomena," Academic Press, New York, 1972.

10. Colburn, A.P., "A Method of Correlating Forced Convection Heat Transfer Data and a Comparison with Fluid Friction," Trans. AIChE, vol. 29, 1933, p. 174.

11. Leach, S.H., and Factor, S.A., "Monitoring Fouling in Refinery and Petrochemical Plant Heat Exchanger," presented at the 20th National Heat Transfer Conference, Milwaukee, Aug. 2-5, 1981.

12. Cowan, J.C. and Weintritt, D.J., "Water Formed Scale Deposits," Gulf Publishing Co., Houston, Texas (1979).

TABLE 1

THERMAL CONDUCTIVITIES OF SCALES AND BIOFILM

	Thermal Conductivity (watt $M^{-1}{}^{\circ}C^{-1}$)
Scale[12]	
Calcium Carbonate	2.26 - 2.93
Calcium Sulfate	2.31
Calcium Phosphate	2.60
Magnesium Phosphate	2.16
Magnetic Iron Oxide	2.88
Analcite	1.27
Biofilm[4,5]	
(Water)	0.63

TABLE 2

FOULING TREATMENT AND CONTROL

	Scaling	Biofouling
External Treatment	Softening Ion exchange	
Internal Treatment	pH control softening acid feed side stream treatment flocculants dispersants surfactants chelants	pH control oxidizing biocides -chlorine -ozone -bromine -hydrogen peroxide non-oxidizing biocides -chlorinated phenolics -organo-tin compounds -quatenary ammonium salt -surfactants
Removal	mechanical cleaning acid treatment	mechanical cleaning oxidizing biocides

Table 3. Summary of the experimental work.

Run	Ca^{++}	Trypticase Soy Broth	Na_2SiO_3	Residence Time	Total Run Time
	ppm	mg/l	mg/l	Hrs	Hrs
1	200	-	-	1	110
2	250	-	-	2	60
3	250	-	200	2	92
4	250	-	-	2	244
5	50	5	-	2	117
6	250	5	-	2	214
7	250	-	200	2	262

TABLE 4

INFLUENCE OF BIOFILMS AND CHEMICAL SCALE DEPOSITS ON FRICTIONAL RESISTANCE.

Type Deposit	Deposit Thickness (μm)	Relative Roughness (Dimensionless)
Biofilms (4)	40	0.003
	165	0.014
	300	0.062
	500	0.157
Scale		
$CaCO_3$	165*	0.0001
	224*	0.0002
	262*	0.0006

* Calculated from overall heat transfer resistance assuming a thermal conductivity for $CaCO_3$ of 0.026 Watts/cm °C

Table 5. Mass analysis of the deposit - Run 7.

Tube sample from	Length# cm	Inside surface area cm^2	Weight of fouled tube*** gm	Weight of clean tube** gm	Mass of deposit gm	Average thickness* μm	Mass per unit length gm/cm	Mass per unit area gm/cm^2
Thickness unit	6.05	24.14	25.3631	25.3458	0.0173	2.54	0.00286	0.00072
Heat transfer measurement block (I)	6.30	25.13	29.8564	29.8386	0.0178	2.45	0.00282	0.00071
Heat transfer measurement block (II)	5.92	23.62	28.1157	28.1011	0.0146	2.20	0.00246	0.00062
Unheated section (I)	6.30	25.13	33.8742	33.8615	0.0127	1.80	0.00200	0.00050
Unheated section (II)	6.00	23.94	32.3114	32.2995	0.0119	1.76	0.00198	0.00050

Tube inside diameter 1.27 cm
** Tube dried at 65 C for 3 hours
* Calculated from dry mass of the deposit assuming uniform deposition. Based on density of calcuim carbonate = 2.82 gm/cm^3

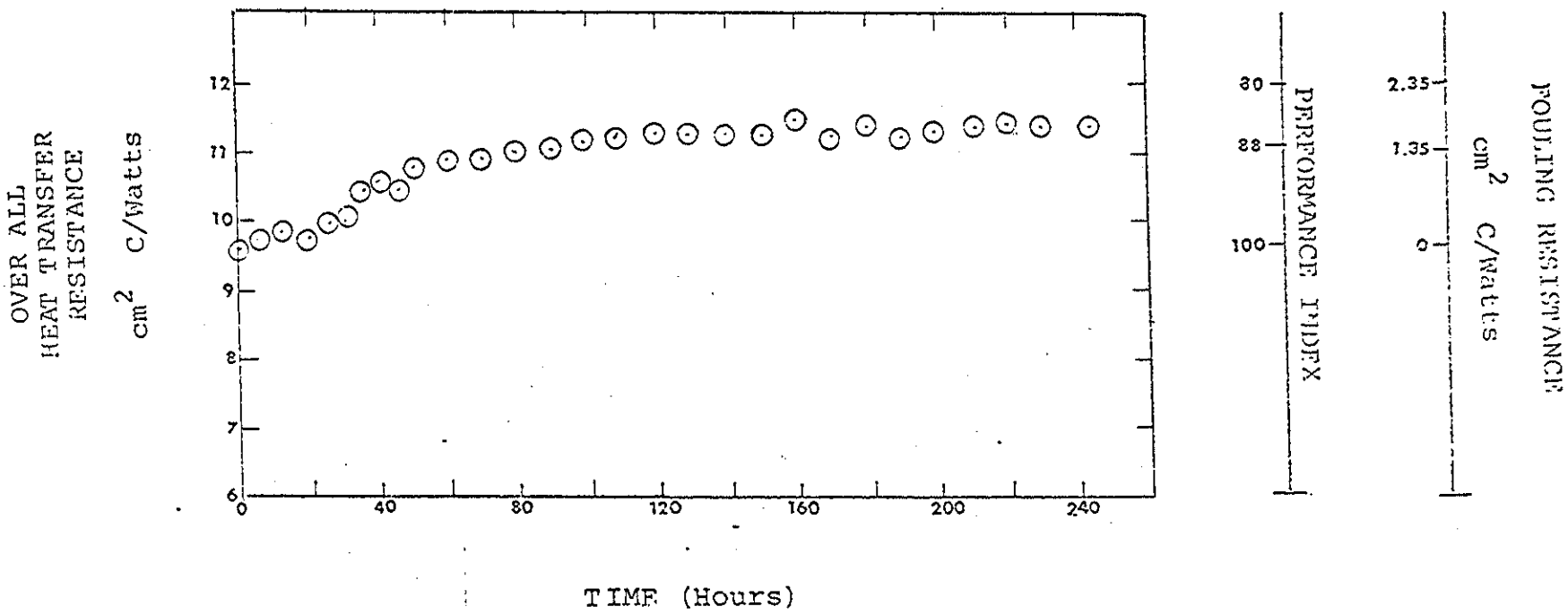

Figure 6. Change in overall heat transfer resistance with time - Run 4.

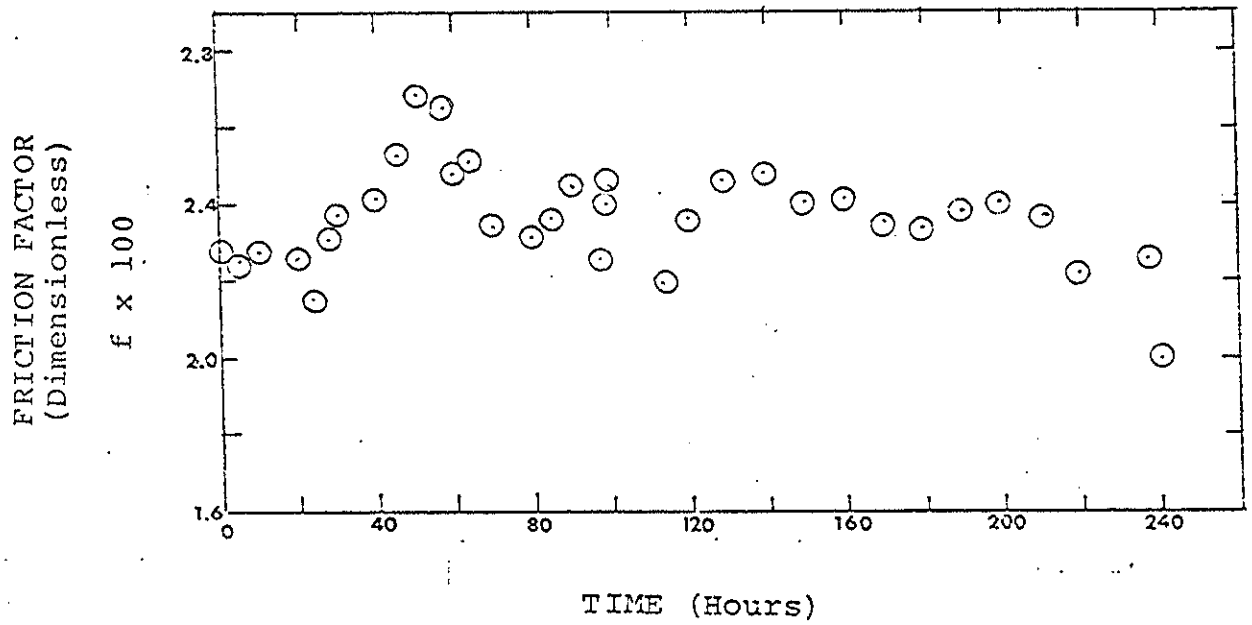

Figure 7. Change in friction factor with time - Run 4.

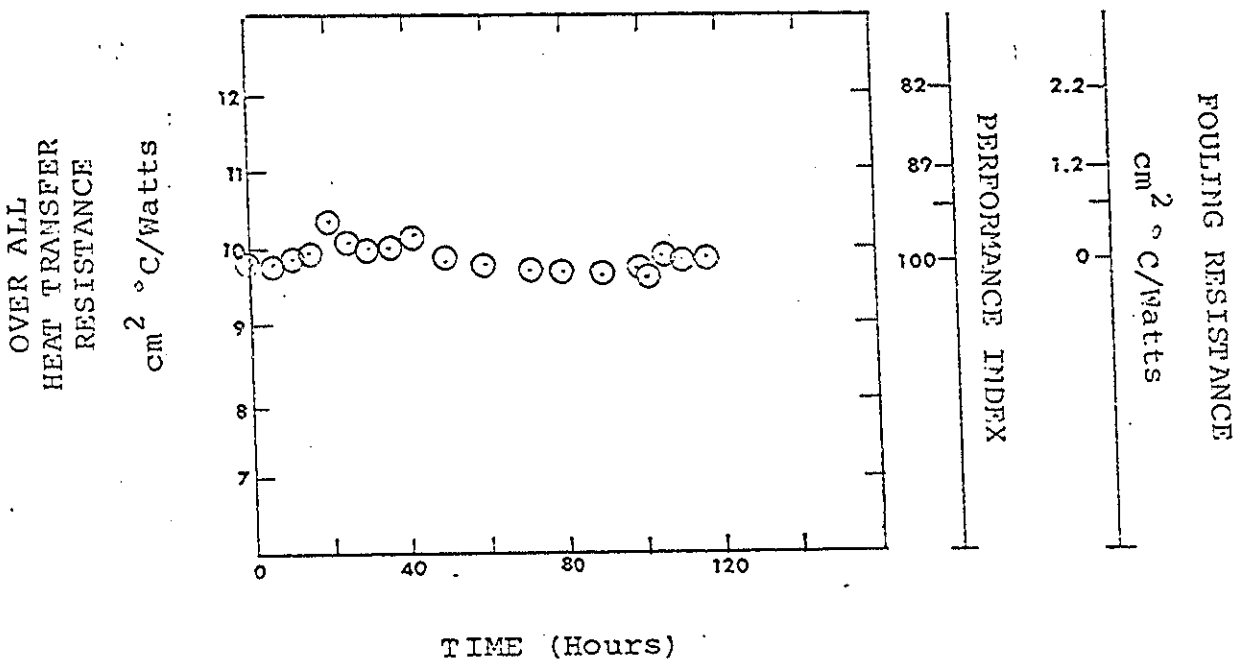

Figure 8. Change in overall heat transfer resistance with time - Run 5.

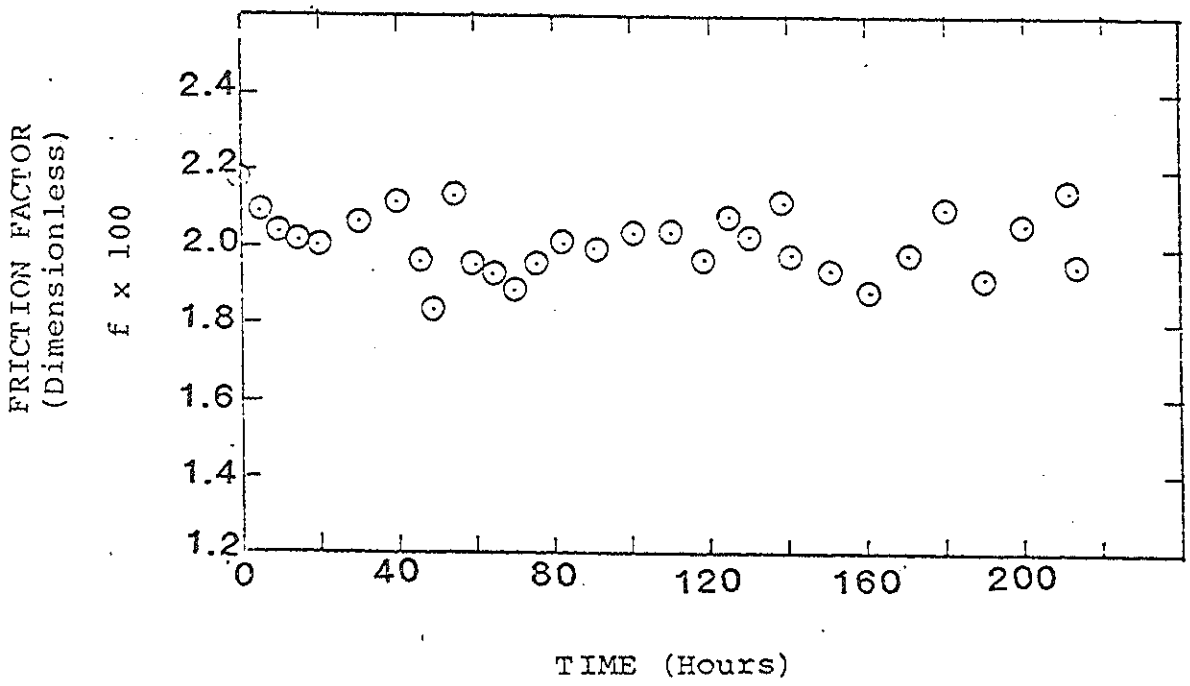

Figure 9. Change in friction factor with time - Run 6.

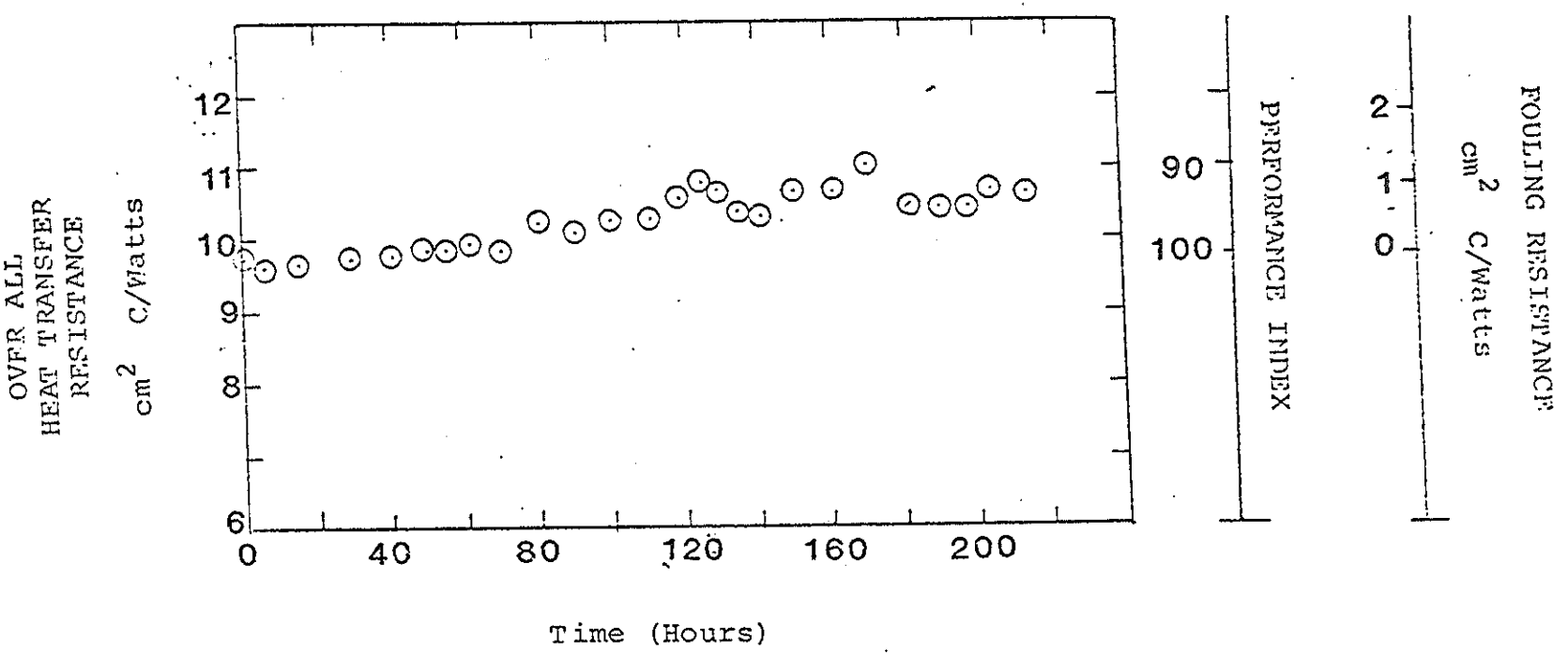

Figure 10. Change in overall heat transfer resistance with time - Run 6.